PNAS RESEARCH ARTICLE | MEDICAL SCIENCES OPEN ACCESS

Impact of repeated blast exposure on active-duty United States Special Operations Forces

Natalie Gilmore[a,b,1], Chieh-En J. Tseng[c,1], Chiara Maffei[a,b,c,1], Samantha L. Tromly[d], Katryna B. Deary[e], Isabella R. McKinney[a,b], Jessica N. Kelemen[a,b], Brian C. Healy[f], Collin G. Hu[g,h], Gabriel Ramos-Llordén[c], Maryam Masood[a,b], Ryan J. Cali[a,b], Jennifer Guo[b], Heather G. Belanger[i], Eveline F. Yao[j], Timothy Baxter[d], Bruce Fischl[c], Andrea S. Foulkes[f], Jonathan R. Polimeni[c], Bruce R. Rosen[c], Daniel P. Perl[k], Jacob M. Hooker[c], Nicole R. Zürcher[c], Susie Y. Huang[c], W. Taylor Kimberly[b], Douglas N. Greve[c], Christine L. Mac Donald[l], Kristen Dams-O'Connor[m,n], Yelena G. Bodien[a,b,o,2], and Brian L. Edlow[a,b,c,2,3]

Edited by Marcus Raichle, Washington University in St. Louis School of Medicine, St. Louis, MO; received August 22, 2023; accepted March 22, 2024

United States (US) Special Operations Forces (SOF) are frequently exposed to explosive blasts in training and combat, but the effects of repeated blast exposure (RBE) on SOF brain health are incompletely understood. Furthermore, there is no diagnostic test to detect brain injury from RBE. As a result, SOF personnel may experience cognitive, physical, and psychological symptoms for which the cause is never identified, and they may return to training or combat during a period of brain vulnerability. In 30 active-duty US SOF, we assessed the relationship between cumulative blast exposure and cognitive performance, psychological health, physical symptoms, blood proteomics, and neuroimaging measures (Connectome structural and diffusion MRI, 7 Tesla functional MRI, [^{11}C]PBR28 translocator protein [TSPO] positron emission tomography [PET]-MRI, and [^{18}F]MK6240 tau PET-MRI), adjusting for age, combat exposure, and blunt head trauma. Higher blast exposure was associated with increased cortical thickness in the left rostral anterior cingulate cortex (rACC), a finding that remained significant after multiple comparison correction. In uncorrected analyses, higher blast exposure was associated with worse health-related quality of life, decreased functional connectivity in the executive control network, decreased TSPO signal in the right rACC, and increased cortical thickness in the right rACC, right insula, and right medial orbitofrontal cortex—nodes of the executive control, salience, and default mode networks. These observations suggest that the rACC may be susceptible to blast overpressure and that a multimodal, network-based diagnostic approach has the potential to detect brain injury associated with RBE in active-duty SOF.

traumatic brain injury | blast overpressure | Special Operations Forces

Significance

We performed a multimodal study of active-duty United States Special Operations Forces (SOF)—an elite group repeatedly exposed to explosive blasts in training and combat—to identify diagnostic biomarkers of brain injury associated with repeated blast exposure (RBE). We found that higher blast exposure was associated with alterations in brain structure, function, and neuroimmune markers, as well as lower quality of life. Neuroimaging findings converged on an association between cumulative blast exposure and the rostral anterior cingulate cortex (rACC), a widely connected brain region that modulates cognition and emotion. This work supports the use of a network-based approach, focusing on the rACC, in future studies investigating the impact of RBE on SOF brain health.

United States (US) Special Operations Forces (SOF) personnel are frequently exposed to explosive blasts in training and combat (1), putting them at risk of brain injury. However, there is currently no diagnostic test to detect brain injury caused by repeated blast exposure (RBE). Without a diagnostic test, SOF personnel may experience cognitive, physical, and psychological symptoms (2) for which the cause is never identified, and they may continue to be exposed to blasts in training or combat during a period of brain vulnerability. There is thus an urgent need to develop a diagnostic test for repeated blast brain injury (rBBI), as early detection of rBBI has the potential to enhance warfighters' combat readiness, career longevity, and quality of life (3).

In this cross-sectional study of active-duty SOF personnel with extensive combat experience and blast exposure in Operations Enduring Freedom, Iraqi Freedom, New Dawn, and Inherent Resolve, we acquired cognitive performance, psychological health, physical symptom, neuroimaging, and blood proteomic measures. Our goals were to elucidate the effects of RBE on SOF brain health and inform the design of a diagnostic testing protocol for rBBI. We pursued a multimodal approach based on the mechanistic complexity of RBE (3, 4), the broad spectrum of candidate biomarkers identified in prior studies (5, 6), and emerging evidence that individual tests may be insufficient to diagnose neurological conditions with heterogeneous pathophysiological subtypes (7).

Results

Demographic and exposure results are provided in Table 1. The 30 male participants were mean (SD) 37.1 (3.9) y old with 17.2 (4.4) y in military service. Combat exposure on the Combat Exposure Scale (CES) (8) was moderate-heavy or heavy in 28 of 30 participants. All participants were exposed to extensive blast overpressure for at least a decade, as determined by the Generalized Blast Exposure Value (GBEV) (2) (Table 1). The range of

The authors declare no competing interest.

This article is a PNAS Direct Submission.

Copyright © 2024 the Author(s). Published by PNAS. This open access article is distributed under Creative Commons Attribution-NonCommercial-NoDerivatives License 4.0 (CC BY-NC-ND).

[1]N.G., C.-E.J.T., and C.M. contributed equally to this work.

[2]Y.G.B. and B.L.E. contributed equally to this work.

[3]To whom correspondence may be addressed. Email: bedlow@mgh.harvard.edu.

This article contains supporting information online at https://www.pnas.org/lookup/suppl/doi:10.1073/pnas.2313568121/-/DCSupplemental.

Published April 22, 2024.

Table 1. Demographics and exposures

Characteristic	SOF participants (n = 30)
Age—y (mean ± SD)	37.1 ± 3.9
Sex: Male—no.	30
Race: White—no.	30
Ethnicity: Non-Hispanic—no.	27
Education—y (mean ± SD)	16.9 ± 2.0
Years in service (mean ± SD)	17.2 ± 4.4
Military branch—no.	20 Army 4 Navy 4 Air Force 2 Marines
Rank—no.	
Officer	1
Warrant Officer	4
Enlisted	25
CES Score (mean ± SD)	33 ± 5.0
Combat Exposure (CES)—no.	
Moderate	2
Moderate-heavy	10
Heavy	18
Surrounded by Enemy—no.	
0 times	1
1 to 2 times	1
3 to 12 times	6
13 to 25 times	3
26+ times	19
Blows to the head (BISQ)—no.	
Low	9
High	21
Cumulative blast exposure (GBEV; median [range])	9,593,890 [387,861 to 363,812,869]
Most recent blast exposure—no.	
<1 y	26
1 y	2
2 y	2

Blows to the head "high" = number of participants with more blows to the head than they could remember; "low" = number of participants who could recall a finite number of blows to the head (range of blows to the head: 1 to 13), assessed by the Brain Injury Screening Questionnaire (BISQ). As an illustration of combat exposure, we provide the "Surrounded by Enemy" Combat Exposure Scale (CES) item results. Abbreviations: GBEV = Generalized Blast Exposure Value; SOF = Special Operations Forces. Enrollment details are provided in *SI Appendix*, Fig. S1.

cumulative exposures for the participants with the lowest (387,861) and highest (363,812,869) GBEV was 67,200 to 224,640 small arms, 270 to 1,260,000 large arms, 240 to 16,200 artillery or missiles carried by vehicle, aircraft, or boat, 648 to 2,550 small explosives, and 11 to 180 large explosives. Twenty-six participants (86.7%) reported that their most recent exposure occurred within the past year, two participants (6.7%) reported that their most recent exposure occurred 1 y ago, and two (6.7%) that their most recent exposure occurred 2 y ago.

A board-certified neuroradiologist and neurologist reviewed all conventional brain MRI scans acquired at the study visit. No acute or chronic traumatic lesions were detected for any of the participants. Thus, none of the participants met Veterans Affairs/Department of Defense (VA/DoD) diagnostic criteria for moderate-severe traumatic brain injury (TBI) (9), consistent with historical information about head trauma provided by participants and medical records review during screening (*SI Appendix*, Tables S1–S3).

From a comprehensive set of cognitive performance, psychological health, physical symptom, neuroimaging, and blood proteomic measures (*SI Appendix*, Table S2), we analyzed measures and brain regions for which an association with cumulative blast exposure was observed in prior studies (*SI Appendix*, Tables S4–S11). The level of cumulative blast exposure was not associated with cognitive performance, blood proteomics, diffusion MRI (dMRI), or tau positron emission tomography (PET) measures (*SI Appendix*, Tables S12–S19). Significant associations between GBEV and measures of psychological health, physical symptoms, functional MRI (fMRI), structural MRI, and translocator protein (TSPO) PET were observed in unadjusted and adjusted linear regression models (Fig. 1 and *SI Appendix*, Table S20). Below we report significant associations from the adjusted linear regression models (i.e., including age, CES score, and blunt head trauma as covariates).

Increased blast exposure was associated with increased cortical thickness in the left rACC (β = 0.67, 95% CI, 0.33 to 1.02), a finding that survived multiple comparison correction (Bonferroni-corrected alpha level = 0.001). At an uncorrected alpha level = 0.05, increased blast exposure was associated with lower scores on the general health subscale of the self-reported RAND-36 Measure of Health-Related Quality of Life (β = −0.45, 95% CI, −0.85 to −0.06), decreased functional connectivity in the executive control network (β = −0.50, 95% CI, −0.92 to −0.07), decreased TSPO signal in the right rACC (β = −0.47, 95% CI, −0.92 to −0.02), and increased cortical thickness in the right rACC (β = 0.50, 95% CI, 0.10 to 0.91), right medial orbitofrontal cortex (β = 0.50, 95% CI, 0.09 to 0.90), and right insula (β = 0.45, 95% CI, 0.03 to 0.87), as shown in Fig. 2. These anatomic regions were functionally connected to the executive control, salience, and default mode networks in group-level analysis of the 7 Tesla (7T) resting-state fMRI data. The rACC was at the intersection of these three distributed networks, as shown in Fig. 3.

To confirm the finding that cumulative blast exposure was positively associated with left rACC cortical thickness (as derived from the T1 multiecho magnetization-prepared rapid gradient-echo [MEMPRAGE] sequence acquired during the Connectome MRI scan), we performed a post hoc analysis using cortical thickness measures derived from the T1 MEMPRAGE sequence acquired

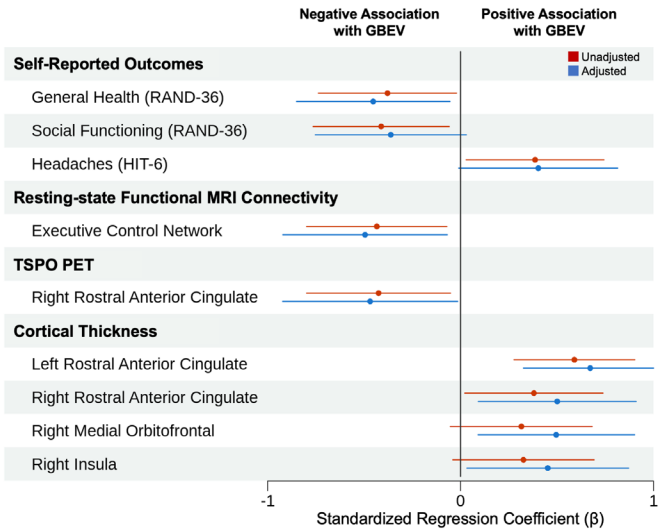

Fig. 1. Blast exposure associations with psychological health, physical symptoms, and neuroimaging measures. We display all measures that showed an association with GBEV in univariate (i.e., unadjusted) or multivariable (i.e., adjusted) analyses. Filled circles represent standardized regression coefficients (β). Solid lines represent 95% CIs. In multivariable analyses, higher GBEV was associated with lower scores on the general health subscale of the RAND-36 Measure of Health-Related Quality of Life, decreased functional connectivity in the executive control network, decreased TSPO signal in the right rACC, and increased cortical thickness in the left rACC, right rACC, right medial orbitofrontal cortex, and right insula. The association between higher GBEV and increased cortical thickness in the left rACC survived correction for multiple comparisons.

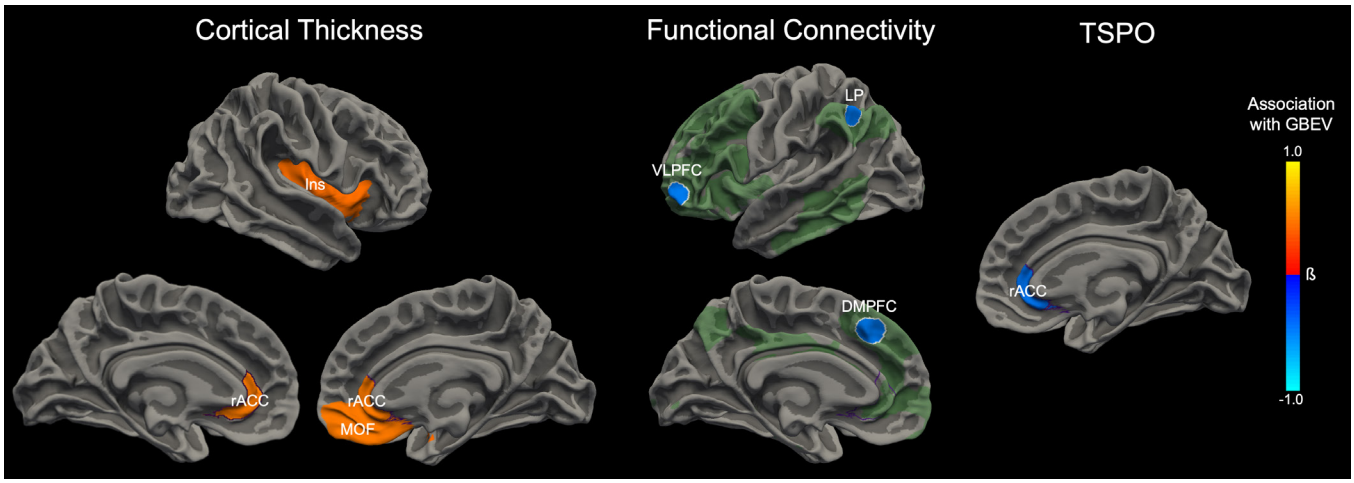

Fig. 2. Associations between blast exposure and neuroimaging measures. Cumulative blast exposure, measured by an interview-based GBEV, was associated with alterations in T1-weighted measures of cortical thickness (*Left*), 7T resting-state fMRI measures of functional connectivity (*Middle*), and PET-MRI measures of TSPO (*Right*). For each modality, the anatomic regions that showed a significant association with GBEV in the adjusted regression models (controlling for age, combat exposure, and blows to the head) are superimposed on the surface of the brain. Orange colors indicate a positive association with GBEV, whereas blue colors represent a negative association with GBEV. The scalar bar color is weighted by the standardized regression coefficient (β). For the functional connectivity analysis, the seed nodes used to assess executive control network connectivity are delineated by white outlines. The extended executive control network derived from the seed nodes is shown in semitransparent green for visualization purposes. The executive control network shown in green represents the mean connectivity derived from the entire cohort. For each neuroimaging measure—cortical thickness, functional connectivity, and TSPO—the associations with GBEV converged on the rACC (outlined in purple). Abbreviations: DMPFC = dorsomedial prefrontal cortex; Ins = insula; MOF = medial orbitofrontal cortex; LP = lateral parietal lobe; VLPFC = ventrolateral prefrontal cortex.

during the PET-MRI scan. In this confirmatory analysis, cumulative blast exposure was positively associated with cortical thickness in the left rACC (β = 0.58, 95% CI, 0.19 to 0.96; *SI Appendix*, Table S21), consistent with the result obtained from the Connectome MRI scan. The T1 MEMPRAGE data obtained during PET-MRI indicated that motion artifact did not contribute to the cortical thickness results, as this T1 MEMPRAGE was acquired with volumetric navigators for prospective motion correction (10).

We also performed post hoc analyses to determine whether post-traumatic stress disorder (PTSD) confounded the association between RBE and the multimodal biomarkers. These analyses were motivated by prior animal (11, 12) and human (13) studies showing associations between PTSD and RBE, as well as human MRI studies suggesting PTSD-related brain alterations in the absence of head trauma (14, 15). The severity of PTSD symptoms, as measured by the PTSD checklist for DSM-5 (PCL-5) score, was not associated with cumulative blast exposure (*SI Appendix*, Table S22). Further, when the PCL-5 score was added to the models with age, combat exposure, and blunt head trauma, the results were similar, suggesting that the associations between blast exposure and cortical thickness, functional connectivity, TSPO signal, and quality of life were likely not attributable to coexisting PTSD symptoms (*SI Appendix*, Tables S12–S20).

Discussion

In 30 active-duty US SOF personnel, higher blast exposure was associated with a decrease in health-related quality of life and brain alterations detected by MRI and PET. Neuroimaging findings converged on an association between cumulative blast exposure and structural, functional, and neuroimmune properties of the rACC, a widely connected frontal lobe region that integrates signaling within the executive control, salience, and default mode networks and modulates cognition and emotion (16). The results did not change after including PTSD symptom severity in the multivariable model, suggesting that PTSD was not driving the relationship between blast exposure and biomarkers in this study. Overall, these observations indicate that RBE may adversely affect SOF brain health and support the use of a network-based approach, focusing on the rACC, in future investigations of rBBI.

Biomechanical studies suggest that the rACC may be susceptible to RBE because of its proximity to overpressure waves entering the intracranial vault via the orbits (17). The rACC also contains von Economo spindle neurons—highly evolved neurons that may be vulnerable to RBE because of their long axonal extensions (18). The left rACC structural imaging finding, which survived correction for multiple comparisons and was replicated using data from a second T1 MEMPRAGE sequence, is consistent with a study of explosive breachers showing an association between blast exposure and increased cortical thickness (6). We and others (6) interpret this finding as reflecting potential injury at the gray-white junction, based on histopathological (19) and neuroimaging (20) evidence for astroglial scarring at this anatomic location.

The correspondence of TSPO signal changes within the rACC suggests a link between neuroimmune function and cortical thickness. We observed a decrease in rACC TSPO signal in the context of an increase in rACC cortical thickness, suggesting that partial volume effects (21) are unlikely to be driving the association between TSPO signal and RBE. While TSPO is highly expressed in reactive microglia and astrocytes, it is also expressed within the mitochondria of neurons, endothelial cells, and vascular smooth muscle cells (22). Thus, our TSPO PET findings within the rACC do not distinguish specific changes in neuroimmune function from broader alterations in cellular metabolism. A key future direction will be to elucidate the pathophysiological mechanisms and temporal dynamics underlying the relationship between neuroimmune function, cellular metabolism, and astroglial scarring at the gray-white matter junction, particularly given emerging evidence of neuroinflammation in SOF personnel (23).

GBEV was not associated with cognitive performance, psychological health, physical symptoms, blood proteomic biomarkers, dMRI, or tau PET in adjusted linear regression analyses. Prior studies suggest that single blast-related mild TBI is associated with some measures in these domains. Our observations add to growing evidence that rBBI is a pathophysiologic entity that is distinct from single blast-related mild TBI (19, 20), just as histopathological (24) and

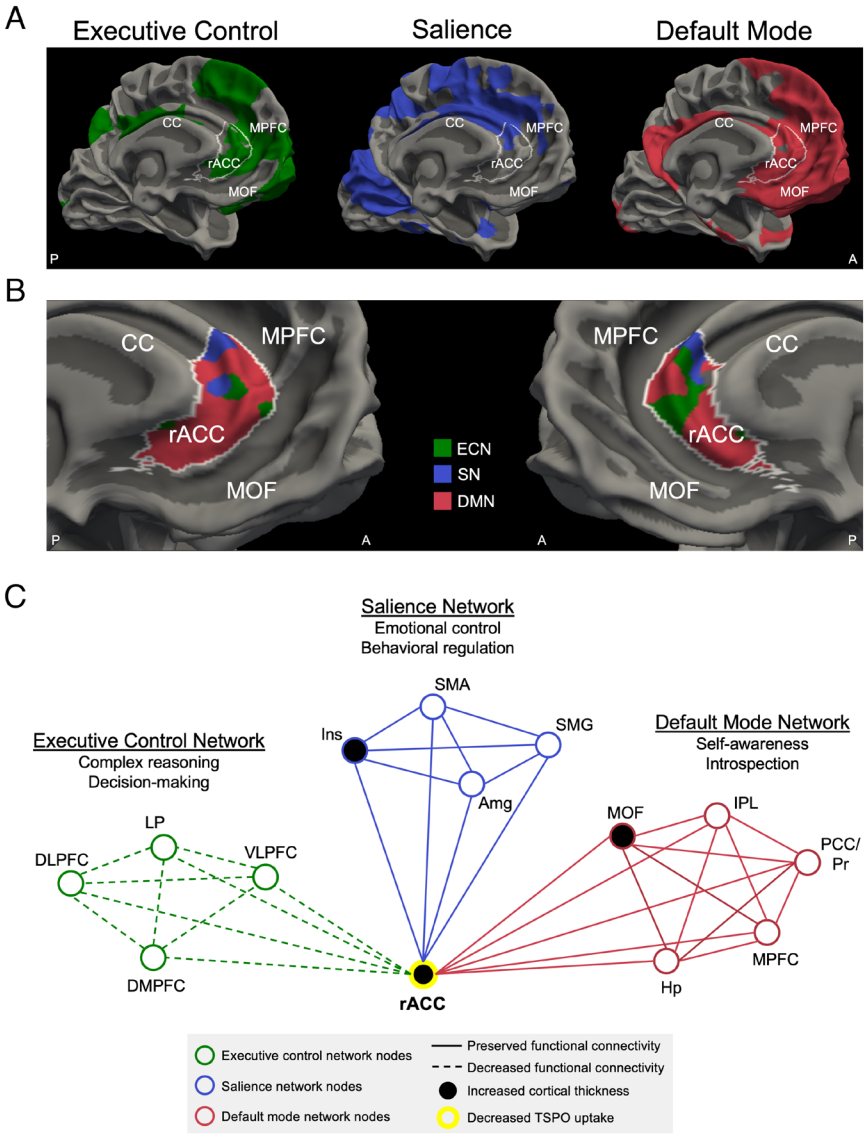

Fig. 3. Brain network alterations associated with cumulative blast exposure. (*A*) The executive control network (ECN, green), salience network (SN, blue), and default mode network (DMN, red) are shown on the medial surface of the left cerebral hemisphere. Each network represents the mean connectivity derived from the entire cohort of 28 participants who had usable 7T resting-state fMRI data. All three networks connect with the rACC, outlined in white, indicating that the rACC is a hub node with functional connectivity to the ECN, SN, and DMN. (*B*) rACC connectivity with the ECN, SN, and DMN is shown on the medial surface of the left and right cerebral hemispheres. rACC vertices on the cortical surface are color-coded according to which network has the highest level of functional connectivity with the rACC at that anatomic location. (*C*) Structural, functional, and neuroimmune alterations are shown in schematic form within the ECN, SN, and DMN. These network alterations converge on the rACC hub node. Abbreviations: A = anterior; Amg = amygdala; CC = corpus callosum; DLPFC = dorsolateral prefrontal cortex; DMPFC = dorsomedial prefrontal cortex; Hp = hippocampus; Ins = insula; IPL = inferior parietal lobule; LP = lateral parietal lobe; MOF = medial orbitofrontal cortex; MPFC = medial prefrontal cortex; P = posterior; PCC/Pr = posterior cingulate cortex/precuneus; SMA = supplementary motor area; SMG = supramarginal gyrus; TSPO = translocator protein; VLPFC = ventrolateral prefrontal cortex. Of note, the Raichle atlas nodes, which were used as seed regions to generate each functional network (as shown in *SI Appendix*, Fig. S2), are a subset of the ECN, SN, and DMN nodes shown in the schematic in (*C*).

neuroimaging (25) studies suggest that chronic traumatic encephalopathy in individuals with repeated subconcussive blunt head trauma is a pathophysiologic entity that is distinct from single blunt mild TBI (3).

The lack of an association between blast exposure and some measures (e.g., cognitive performance, PTSD symptoms, blood proteomics) may be attributable to a restricted range for the GBEV variable, as scores for all 30 active-duty US SOF participants exceeded previously published levels (2). Similarly, high blood tau and p-tau levels may have further masked a relationship between blood proteomics and blast exposure. In our sample, blood tau levels were ten times higher and p-tau levels were 1.5 times higher than those previously reported in breacher trainees exposed to two consecutive days of blasts (tau = 3.69 versus 0.33 pg/mL; p-tau = 1.56 versus 1.13 pg/mL, *SI Appendix*, Table S14) (26). Given these limitations and that cognitive and blood biomarkers are feasible to acquire in austere combat environments, further investigation is warranted to determine the diagnostic utility of these measures.

Several additional limitations should be considered when interpreting the study results. The GBEV has not been validated against blast gauge data as a tool for estimating blast exposure. Its precision, accuracy, and potential susceptibility to recall bias are areas of ongoing investigation (27). The GBEV also reports the recency of blast exposure in units of years, not days or weeks. All but four participants reported that their most recent blast exposure occurred within 1 y of study participation, suggesting minimal variability in exposure timing across the sample. Therefore, we were unable to determine the relative contributions

of chronic versus acute blast exposure to the observed biomarker changes.

The absence of a control cohort in this study reflects the challenge of identifying blast-naïve military personnel who perform at the elite cognitive and physical levels of active-duty SOF. We also did not measure the myriad exposures experienced by SOF that may affect their brain structure and function, including high-altitude jumping, deep sea diving, inhalation of heavy metal fumes, noise exposure, aircraft vibrations, and g-forces while traveling over tall waves at high speeds (3). We were unable to include a continuous measure of lifetime frequency of blunt head trauma as a covariate (28) because 70% of the sample reported more blows to the head than they could remember. The small sample size of 30 participants in the context of a large battery of measures likely contributed to only one finding (the association between higher GBEV and increased cortical thickness in the left rACC) surviving correction for multiple comparisons. Finally, while PTSD symptoms did not affect the relationship between blast exposure and cortical thickness, TSPO signal, functional connectivity, or quality of life, the PCL-5 has limitations associated with being a self-report measure (29). Future studies may consider using clinician-rated measures to assess PTSD symptoms.

In summary, we observed that RBE is associated with lower health-related quality of life and brain alterations detectable by MRI and PET in active-duty US SOF. These alterations affected the executive control, salience, and default mode networks, with the strongest line of evidence indicating that the rACC hub node in the frontal lobe is susceptible to RBE. Future efforts to develop a diagnostic testing protocol for rBBI should consider a network-based approach focusing on the rACC to optimize SOF brain health.

Materials and Methods

The ReBlast (Long-term Effects of RBE in US SOF Personnel) study protocol was approved by the Mass General Brigham Institutional Review Board (2020P002695) and registered at ClinicalTrials.gov (NCT05183087). Data acquisition protocols and the prespecified statistical plan were previously described in detail (30).

Subjects. Screening was performed in coordination with US Special Operations Command (USSOCOM) personnel who disseminated recruitment fliers via email lists. Inclusion criteria were 1) male; 2) age 25 to 45 y; 3) active-duty SOF; 4) prior combat deployment; 5) prior combat exposure during deployment, verified by the CES (8); and 6) exposure to blast overpressure, verified by the GBEV (2). We excluded participants with 1) moderate-severe TBI; and 2) imaging contraindication (see *SI Appendix*, Table S1 for complete exclusion list). All participants agreed to participate in writing before study procedures were initiated, in accordance with informed consent procedures.

SOF personnel traveled to the Massachusetts General Hospital Athinoula A. Martinos Center for Biomedical Imaging for 2 d and participated in 12 h of cognitive performance, psychological health, and physical symptom assessments, four brain scans (3T Connectome MRI, 7T MRI, [^{11}C]PBR28 TSPO PET-MRI, and [^{18}F]MK6240 tau PET-MRI) and blood acquisition for proteomic analysis (*SI Appendix*, Fig. S1 and Table S2).

Blast, Combat, and Blunt Mild TBI Exposure. We measured blast exposure using an interview-based version of the GBEV (2) administered by a study investigator in the SOF community. The GBEV provides a unitless value of cumulative blast exposure derived by applying weighting factors to average frequencies of lifetime exposure to 1) small/medium arms (e.g., rifles, machine guns); 2) large arms (e.g., shoulder-carried rocket-propelled weapon systems); 3) artillery or missiles carried by vehicle, aircraft, or boat; 4) small explosives (e.g., grenades, flashbangs, small improvised explosive devices [IEDs]); and 5) large explosives (e.g., breaching explosives, large IEDs). The final question of the GBEV asks about recency of blast exposure (i.e., <1 y, 1 y or more, and if 1 y or more, the number of years since last exposure). We log-transformed the GBEV to account for the non-normal distribution of scores.

Participants completed the CES, for which the total score represents overall combat exposure. They also completed the interview-based Brain Injury Screening Questionnaire (BISQ) to capture lifetime exposure to TBI. As a part of this comprehensive TBI screening, participants were asked whether they had ever experienced a blow to the head in over 20 different situations (e.g., combative training and contact sports) (28). All participants endorsed at least one blow to the head and 21 participants endorsed more blows to the head than they could remember. Although the BISQ typically asks whether each blow to the head was followed by altered mental status (i.e., loss of consciousness, dazed and confused), we only asked about altered mental status for the three worst events, because participants frequently were unable to recall a finite number of blows to the head. All participants endorsed at least one blow to the head with either alteration of consciousness or loss of consciousness, consistent with mild TBI, as defined by the VA/DoD (9).

Given that we could not quantify the total number of mild TBIs, to account for head trauma we generated a dichotomous variable using participants' report of lifetime blows to the head. Participants in the "high incidence" blunt head trauma group (n = 21) had more blows to the head than they could remember, primarily due to repeated exposures during combative training and contact sports. Participants in the "low incidence" blunt head trauma group (n = 9) recalled a finite number of blows to the head (range 1 to 13). Thus, in addition to the CES total score and age, we included blows to the head as a covariate in multivariable (i.e., adjusted) linear regressions.

Cognitive Performance, Psychological Health, and Physical Symptoms. The cognitive performance battery tested executive function, attention, learning and memory, processing speed, and visuospatial processing (*SI Appendix*, Table S3). In addition to standard paper-and-pencil cognitive assessments, we administered the computer-based Automated Neuropsychological Assessment Metrics (ANAM) (31) and the iPad-based Philips IntelliSpace Cognition (32) tests. In the week prior to and during the study visit, participants also completed self-report measures assessing psychological health and physical symptoms, as previously described (30). Scores on cognitive performance and self-report symptom measures were assessed for validity in one of two ways depending on the measure: 1) comparison to standard cutoffs on stand-alone measures [i.e., Mild Brain Injury Atypical Symptoms (33), Medical Symptom Validity Test (34)]; or 2) automated evaluation of effort via metrics embedded in the assessment (i.e., ANAM, Philips IntelliSpace Cognition). Performance validity and symptom validity were confirmed for all measures and thus, no cognitive performance or self-reported symptom data were removed before analysis. See *SI Appendix* for additional details.

Blood Proteomics. Blood samples were collected from fasted participants and centrifuged immediately. The plasma was aliquoted and stored at −80 °C until analysis. We used Simoa Human Neurology 4-Plex A (N4PA), 3-Plex A (N3PA), and pTau181 assays at the Simoa Accelerator Laboratory (Quanterix, Billerica, MA) to measure plasma protein levels: neurofilament light (NfL), phosphorylated tau181 (p-tau), tau, ubiquitin carboxyl-terminal esterase L1 (UCH-L1), amyloid beta 40 (Aβ40), amyloid beta 42 (Aβ42), and glial fibrillary acidic protein.

Neuroimaging Data Acquisition. Participants were scanned with 7T MRI for functional connectivity analysis, 3T Connectome MRI for diffusion and volumetric analyses, [^{11}C]PBR28 TSPO PET-MRI for analysis of TSPO, a mitochondrial protein involved in neuroimmune function, and [^{18}F]MK6240 tau PET-MRI for analysis of neurofibrillary tangles. Acquisition parameters are described in *SI Appendix* and have been previously published (30).

Resting-State Functional MRI. Blood-oxygenation-level-dependent (BOLD) data were acquired on a 7T Terra MRI scanner (Siemens Healthineers, Erlangen, Germany) with a 32-channel head coil (Nova Medical, Wilmington, MA). BOLD data were processed in the FreeSurfer 7.3.0 Functional Analysis Stream (FSFAST) (35) for B_0 distortion correction, motion correction, slice-timing correction, and temporal detrending. Functional networks were identified using Raichle atlas network nodes as seed regions (*SI Appendix*, Fig. S2) (36). The anatomic coordinates of network nodes were projected onto the surface of the cerebral cortex as discs with a 10 mm radius (allowing the mean waveform to be computed exclusively in cortical gray matter), or onto subcortical structures as spheres with a 10 mm radius. Functional connectivity was measured by averaging the BOLD

signal within each node, deriving a Pearson correlation coefficient between each pair of nodes, and then averaging the Pearson correlation coefficients across all nodes in each network.

dMRI. dMRI data were acquired on a 3T Connectome scanner (MAGNETOM CONNECTOME Siemens Healthineers, Erlangen, Germany) using a 64-channel custom-made head coil (37). Data preprocessing included correction for gradient nonlinearity distortions and susceptibility-induced distortions, head motion, and eddy-current-induced artifacts (38). Reconstruction of selected white matter pathways was performed automatically using the global probabilistic tractography algorithm TRACULA in FreeSurfer 7.3.0 (*SI Appendix*, Fig. S3) (39). White matter integrity was measured as the weighted average of fractional anisotropy across all voxels within each pathway.

[^{11}C]PBR28 TSPO and [^{18}F]MK6240 Tau PET-MRI. [^{11}C]PBR28 TSPO and [^{18}F]MK6240 tau PET data were acquired on a hybrid PET–MRI scanner, the Siemens BrainPET, which is based on a head-only PET camera inserted into the bore of a 3T TIMTrio MRI scanner (40). A T1-weighted structural scan was also acquired using MEMPRAGE at 1 mm isotropic resolution with prospective motion correction (41). The emission data collected from 60 to 90 min post-radioligand injection for [^{11}C]PBR28 and 70 to 90 min post-radioligand injection for [^{18}F]MK6240 were divided into 5-min frames, reconstructed to standardized uptake value (SUV) images using an MRI-based attenuation map (described in *SI Appendix*), realigned (42) and averaged. The SUV image was then linearly registered to the participant's T1-weighted MEMPRAGE scan using FreeSurfer's spmregister [version 5.3, the version that is most accurate for registering PET to MRI data (43)], skull-stripped, and normalized by a pseudo-reference region ([^{11}C]PBR28: whole brain without ventricles (43), [^{18}F]MK6240: isthmus cingulate cortex (44)) to account for individual differences in global signal (SUVR). Individuals with a TSPO genotype that confers low-affinity binding for [^{11}C]PBR28 were excluded from the TSPO PET analyses (*SI Appendix*, Table S23).

Cortical Thickness. T1-weighted structural MRI data were acquired on the Connectome scanner using the same hardware as the dMRI acquisition. Data were corrected for gradient nonlinearity distortions and processed in FreeSurfer 7.3.0 using the automated "recon-all" pipeline (45) and the Desikan–Killiany atlas (46) to parcellate the cerebral cortex for thickness analysis (*SI Appendix*, Fig. S4).

Statistical Analysis. We performed univariate (i.e., unadjusted) and multivariable (i.e., adjusted for age, combat exposure, and blunt head trauma) linear regression using log-transformed GBEV as a continuous variable to predict each measure. We report standardized regression coefficients (β) to quantify the magnitude of the effect and to compare results across measures. We applied Bonferroni correction for multiple comparisons. In post hoc analyses, we tested the association between cortical thickness measures derived from the T1 MEMPRAGE sequence acquired during the PET-MRI scan and cumulative blast exposure using log-transformed GBEV. We also tested the association between PTSD symptom severity, as measured by the PCL-5 score, and cumulative blast exposure. We performed an additional set of multivariable regression analyses adjusting for age, combat exposure, blunt head trauma, and PTSD symptom severity. See *SI Appendix* for details on data quality assessments conducted for each measure and for the results of additional statistical analyses (*SI Appendix*, Tables S12–S24).

Data, Materials, and Software Availability. USSOCOM regulations prevent public release of the data generated for this study. Future requests for these data may be submitted to the corresponding author and will then need to be vetted by USSOCOM. All T1-weighted MEMPRAGE data and BOLD fMRI data were processed using a standard release of FreeSurfer available at https://github.com/freesurfer/freesurfer (35). The dMRI, TSPO PET-MRI, and tau PET-MRI data were processed using a combination of tools: FreeSurfer (including TRACULA) available at the aforementioned github link and FSL available at https://fsl.fmrib.ox.ac.uk/fsl/fslwiki (47).

ACKNOWLEDGMENTS. This study was funded by the US Department of Defense (USSOCOM Contract No. H9240520D0001). We thank the Navy SEAL Foundation for their support of this work. We are grateful to the 30 individuals who participated in the study. The views expressed in this manuscript are entirely those of the authors and do not necessarily reflect the views, policy, or position of the United States Government, Department of Defense, USSOCOM, or the Uniformed Services University of the Health Sciences.

Author affiliations: [a]Center for Neurotechnology and Neurorecovery, Massachusetts General Hospital, Boston, MA 02114; [b]Department of Neurology, Massachusetts General Hospital and Harvard Medical School, Boston, MA 02114; [c]Department of Radiology, Athinoula A. Martinos Center for Biomedical Imaging, Massachusetts General Hospital and Harvard Medical School, Charlestown, MA 02129; [d]Institute of Applied Engineering, University of South Florida, Tampa, FL 33612; [e]Navy SEAL Foundation, Virginia Beach, VA 23455; [f]Harvard T.H. Chan School of Public Health, Boston, MA 02115; [g]United States Army Special Operations Aviation Command, Fort Liberty, NC 28307; [h]Department of Family Medicine, F. Edward Hebert School of Medicine, Uniformed Services University of the Health Sciences, Bethesda, MD 20814; [i]Department of Psychiatry and Behavioral Neurosciences, University of South Florida, Tampa, FL 33613; [j]Office of the Air Force Surgeon General, Falls Church, VA 22042; [k]Department of Pathology, F. Edward Hébert School of Medicine, Uniformed Services University of the Health Sciences, Bethesda, MD 20814; [l]Department of Neurological Surgery, University of Washington, Seattle, WA 98195; [m]Department of Rehabilitation and Human Performance, Icahn School of Medicine at Mount Sinai, New York, NY 10029; [n]Department of Neurology, Icahn School of Medicine at Mount Sinai, New York, NY 10029; and [o]Department of Physical Medicine and Rehabilitation, Spaulding Rehabilitation Hospital and Harvard Medical School, Charlestown, MA 02129

Author contributions: S.L.T., B.C.H., M.M., H.G.B., E.F.Y., T.B., B.F., A.S.F., J.R.P., B.R.R., D.P.P., J.M.H., N.R.Z., S.Y.H., W.T.K., D.N.G., C.L.M.D., K.D.-O., Y.G.B., and B.L.E. designed research; N.G., C.-E.J.T., C.M., K.B.D., I.R.M., J.N.K., C.G.H., G.R.-L., R.J.C., J.G., Y.G.B., and B.L.E. performed research; N.G., C.-E.J.T., C.M., I.R.M., B.C.H., G.R.-L., J.G., N.R.Z., S.Y.H., W.T.K., D.N.G., Y.G.B., and B.L.E. analyzed data; S.L.T., I.R.M., J.N.K., M.M., and T.B. material support; and N.G., C.-E.J.T., C.M., Y.G.B., and B.L.E. wrote the paper.

1. A. Garcia *et al.*, Health conditions among Special Operations Forces versus conventional military service members: A VA TBI model systems study. *J. Head Trauma Rehabil.* **37**, E292–E298 (2022).
2. L. C. M. Modica, M. J. Egnoto, J. K. Statz, W. Carr, S. T. Ahlers, Development of a blast exposure estimator from a department of defense-wide survey study on military service members. *J. Neurotrauma* **38**, 1654–1661 (2021).
3. B. L. Edlow *et al.*, Optimizing brain health of United States Special Operations Forces. *J. Spec. Oper. Med.* **23**, 47–56 (2023).
4. J. V. Rosenfeld *et al.*, Blast-related traumatic brain injury. *Lancet Neurol.* **12**, 882–893 (2013).
5. C. L. Mac Donald *et al.*, Detection of blast-related traumatic brain injury in U.S. military personnel. *N. Engl. J. Med.* **364**, 2091–2100 (2011).
6. J. R. Stone *et al.*, Functional and structural neuroimaging correlates of repetitive low-level blast exposure in career breachers. *J. Neurotrauma* **37**, 2468–2481 (2020).
7. B. M. Asken *et al.*, Multi-modal biomarkers of repetitive head impacts and traumatic encephalopathy syndrome: A clinicopathological case series. *J. Neurotrauma* **39**, 1195–1213 (2022).
8. T. M. Keane *et al.*, Clinical evaluation of a measure to assess combat exposure. *Psychol. Assess.* **1**, 53–55 (1989).
9. The Management of Concussion-Mild Traumatic Brain Injury Working Group, VA/DoD Clinical Practice Guideline for the Management of Concussion-Mild Traumatic Brain Injury (Version 2.0, 2016). https://www.healthquality.va.gov/guidelines/rehab/mtbi/mtbicpgfullcpg50821816.pdf. Accessed 8 January 2024.
10. M. D. Tisdall *et al.*, Volumetric navigators for prospective motion correction and selective reacquisition in neuroanatomical MRI. *Magn. Reson. Med.* **68**, 389–399 (2012).
11. G. A. Elder *et al.*, Blast exposure induces post-traumatic stress disorder-related traits in a rat model of mild traumatic brain injury. *J. Neurotrauma* **29**, 2564–2575 (2012).
12. G. Perez Garcia *et al.*, Progressive cognitive and post-traumatic stress disorder-related behavioral traits in rats exposed to repetitive low-level blast. *J. Neurotrauma* **38**, 2030–2045 (2021).
13. J. N. Belding, C. A. Kolaja, R. P. Rull, D. W. Trone, Single and repeated high-level blast, low-level blast, and new-onset self-reported health conditions in the U.S. Millennium Cohort Study: An exploratory investigation. *Front. Neurol.* **14**, 1110717 (2023).
14. A. Kunimatsu, K. Yasaka, H. Akai, N. Kunimatsu, O. Abe, MRI findings in posttraumatic stress disorder. *J. Magn. Reson. Imaging* **52**, 380–396 (2020).
15. A. N. Simmons, S. C. Matthews, Neural circuitry of PTSD with or without mild traumatic brain injury: A meta-analysis. *Neuropharmacology* **62**, 598–606 (2012).
16. W. Tang *et al.*, A connectional hub in the rostral anterior cingulate cortex links areas of emotion and cognitive control. *Elife* **8**, e43761 (2019).
17. A. Nakagawa *et al.*, Mechanisms of primary blast-induced traumatic brain injury: Insights from shock-wave research. *J. Neurotrauma* **28**, 1101–1119 (2011).
18. J. M. Allman *et al.*, The von Economo neurons in the frontoinsular and anterior cingulate cortex. *Ann. N. Y. Acad. Sci.* **1225**, 59–71 (2011).
19. S. B. Shively *et al.*, Characterisation of interface astroglial scarring in the human brain after blast exposure: A post-mortem case series. *Lancet Neurol.* **15**, 944–953 (2016).
20. D. Benjamini, D. S. Priemer, D. P. Perl, D. L. Brody, P. J. Basser, Mapping astrogliosis in the individual human brain using multidimensional MRI. *Brain* **146**, 1212–1226 (2023).
21. D. N. Greve *et al.*, Different partial volume correction methods lead to different conclusions: An (18) F-FDG-PET study of aging. *Neuroimage* **132**, 334–343 (2016).
22. T. Notter, J. M. Coughlin, A. Sawa, U. Meyer, Reconceptualization of translocator protein as a biomarker of neuroinflammation in psychiatry. *Mol. Psychiatry* **23**, 36–47 (2018).
23. J. R. Stone *et al.*, Neurological effects of repeated blast exposure in special operations personnel. *J. Neurotrauma*, 10.1089/neu.2023.0309 (2024).

24. A. C. McKee *et al.*, The spectrum of disease in chronic traumatic encephalopathy. *Brain* **136**, 43–64 (2013).
25. R. A. Stern *et al.*, Tau positron-emission tomography in former national football league players. *N. Engl. J. Med.* **380**, 1716–1725 (2019).
26. R. Vorn, R. Naunheim, C. Lai, C. Wagner, J. M. Gill, Elevated axonal protein markers following repetitive blast exposure in military personnel. *Front. Neurosci.* **16**, 853616 (2022).
27. S. M. Turner, S. S. Sloley, J. M. Bailie, I. Babakhanyan, E. Gregory, Perspectives on development of measures to estimate career blast exposure history in service members and veterans. *Front. Neurol.* **13**, 835752 (2022).
28. K. Dams-O'Connor *et al.*, Screening for traumatic brain injury: Findings and public health implications. *J. Head Trauma Rehabil.* **29**, 479–489 (2014).
29. M. J. Bovin, B. P. Marx, The problem with overreliance on the PCL-5 as a measure of PTSD diagnostic status. *Clin. Psychol.: Sci. Practice* **30**, 122–125 (2023).
30. B. L. Edlow *et al.*, Long-term effects of repeated blast exposure in United States Special Operations Forces personnel: A pilot study protocol. *J. Neurotrauma* **39**, 1391–1407 (2022).
31. A. S. Vincent, T. Roebuck-Spencer, K. Gilliland, R. Schlegel, Automated neuropsychological assessment metrics (v4) traumatic brain injury battery: Military normative data. *Mil. Med.* **177**, 256–269 (2012).
32. S. Vermeent, M. Spaltman, G. van Elswijk, J. B. Miller, B. Schmand, Philips IntelliSpace Cognition digital test battery: Equivalence and measurement invariance compared to traditional analog test versions. *Clin. Neuropsychol.* **36**, 2278–2299 (2022).
33. R. D. Vanderploeg *et al.*, Screening for postdeployment conditions: Development and cross-validation of an embedded validity scale in the neurobehavioral symptom inventory. *J. Head Trauma Rehabil.* **29**, 1–10 (2014).
34. P. Green, *Green's Medical Symptom Validity Test (MSVT) for Microsoft Windows: User's Manual* (Green's Publishing, Edmonton, Canada, 2004).
35. B. Fischl, FreeSurfer. *Neuroimage* **62**, 774–781 (2012).
36. M. E. Raichle, The restless brain. *Brain Connect.* **1**, 3–12 (2011).
37. B. Keil *et al.*, A 64-channel 3T array coil for accelerated brain MRI. *Magn. Reson. Med.* **70**, 248–258 (2013).
38. J. L. R. Andersson, S. N. Sotiropoulos, An integrated approach to correction for off-resonance effects and subject movement in diffusion MR imaging. *Neuroimage* **125**, 1063–1078 (2016).
39. C. Maffei *et al.*, Using diffusion MRI data acquired with ultra-high gradient strength to improve tractography in routine-quality data. *Neuroimage* **245**, 118706 (2021).
40. A. Kolb *et al.*, Technical performance evaluation of a human brain PET/MRI system. *Eur. Radiol.* **22**, 1776–1788 (2012).
41. M. D. Tisdall *et al.*, Prospective motion correction with volumetric navigators (vNavs) reduces the bias and variance in brain morphometry induced by subject motion. *Neuroimage* **127**, 11–22 (2016).
42. M. Jenkinson, P. Bannister, M. Brady, S. Smith, Improved optimization for the robust and accurate linear registration and motion correction of brain images. *Neuroimage* **17**, 825–841 (2002).
43. N. R. Zurcher *et al.*, [(11)C]PBR28 MR-PET imaging reveals lower regional brain expression of translocator protein (TSPO) in young adult males with autism spectrum disorder. *Mol. Psychiatry* **26**, 1659–1669 (2021).
44. M. E. Robinson *et al.*, Positron emission tomography of tau in Iraq and Afghanistan Veterans with blast neurotrauma. *Neuroimage Clin.* **21**, 101651 (2019).
45. B. Fischl, M. I. Sereno, A. M. Dale, Cortical surface-based analysis. II: Inflation, flattening, and a surface-based coordinate system. *Neuroimage* **9**, 195–207 (1999).
46. R. S. Desikan *et al.*, An automated labeling system for subdividing the human cerebral cortex on MRI scans into gyral based regions of interest. *Neuroimage* **31**, 968–980 (2006).
47. S. M. Smith *et al.*, Advances in functional and structural MR image analysis and implementation as FSL. *Neuroimage* **23**, S208–S219 (2004).